Objectives and Design of the JT-60 Superconducting Tokamak

S. Ishida[1)], K. Abe[2)], A. Ando[2)], T. Cho[3)], T. Fujii[1)], T. Fujita[1)], S. Goto[4)], K. Hanada[5)], A. Hatayama[6)], T. Hino[7)], H. Horiike[4)], N. Hosogane[1)], M. Ichimura[3)], S. Tsuji-Iio[8)], S. Itoh[5)], Y. Kamada[1)], M. Katsurai[9)], M. Kikuchi[1)], A. Kitsunezaki[1)], A. Kohyama[10)], H. Kubo[1)], M. Kuriyama[1)], M. Matsukawa[1)], M. Matsuoka[11)], Y. Miura[1)], Y.M. Miura[1)], N. Miya[1)], T. Mizuuchi[10)], Y. Murakami[12)], K. Nagasaki[10)], H. Ninomiya[1)], N. Nishino[13)], Y. Ogawa[9)], K. Okano[14)], T. Ozeki[1)], M. Saigusa[15)], M. Sakamoto[5)], A. Sakasai[1)], M. Satoh[1)], M.Shimada[16)], R. Shimada[8)], M. Shimizu[1)], T. Takagi[2)], Y. Takase[9)], S. Takeji[1)], T. Tanabe[17)], K. Toi[18)], Y. Ueda[4)], Y. Uesugi[16)], K. Ushigusa[1)], M. Wakatani[10)], Y. Yagi[19)], K. Yamaguchi[1)], T. Yamamoto[1)], K. Yatsu[3)], and K. Yoshikawa[10)]

1) Japan Atomic Energy Research Institute, 2) Tohoku University, 3) University of Tsukuba, 4) Osaka University, 5) Kyushu University, 6) Keio University, 7) Hokkaido University, 8) Tokyo Institute of Technology, 9) the University of Tokyo, 10) Kyoto University, 11) Mie University, 12) Toshiba Corporation Power Systems and Services Company, 13) Hiroshima University, 14) Central Research Institute of Electric Power Industry, 15) Ibaraki University, 16) ITER JCT, 17) Nagoya University, 18) National Institute for Fusion Science, 19) National Institute of Advanced Industrial Science and Technology, Japan

e-mail contact of main author: ishida@naka.jaeri.go.jp

Abstract. A fully superconducting tokamak named as JT-60SC is designed for the modification program of JT-60 to enhance economical and environmental attractiveness in tokamak fusion reactors. JT-60SC aims at realizing high-beta steady-state operation in the use of low radio-activation ferritic steel in low ν^* and ρ^* regime relevant to the reactor plasmas. Objectives, research issues, plasma control schemes and a conceptual design for JT-60SC are presented.

1. Objectives

The modification program of JT-60 viewing the next decade is oriented in the following directions and a conceptual design of the modification is presented in nation-wide collaboration with universities, institutes and industries. In order to improve economic and environmental suitability of tokamak fusion reactors, the accomplishment of low circulating power operation in accord with a high pressure plasma (i.e., high-beta steady-state operation) [1] and the establishment of utilization technology of low radio-activation materials to minimize the influence of radioactive waste to the environment [2] are crucially important. It is the demonstration of the use of low activation ferritic steel for reactor-relevant plasmas that are necessary to expedite the practical use of the material as a most promising candidate for the first wall material in DEMO reactors. The attainment of these objectives by modifying the JT-60 would effectively contribute to earlier realization of tokamak fusion reactors in cooperation with the ITER program and material developments.

So far, the JT-60 program has consistently pursued the subjects for the basis of steady-state tokamak operation and pioneered advanced tokamak operation regimes consistent with a high bootstrap current fraction such as high-β_p and reversed shear discharges [3]. Thus, the modified JT-60 is oriented to lead the way to demonstrate the high-beta steady-state operation in the use of the ferritic steel characterized by ferromagnetic properties to the plasma confinement device for the reactor-relevant plasmas.

2. Research Issues and Main Parameters

Scale of the plasma to be modified is discussed as follows. It is important for close extrapolation to perform demonstration experiments in steady state bringing non-dimensional parameters of normalized Larmor radius ρ^*, normalized collisionality ν^* and normalized beta β_N closely to those of reactor plasmas. Considering these non-dimensional parameters, the concept of the modification is determined to be a large superconducting tokamak, here called JT-60SC, which allows to create high performance plasmas in a break-even class (DT-equivalent fusion energy multiplication factor $Q_{DT}^{eq} \sim 1$) and to sustain the plasmas for a long

duration (~ 100 s) sufficiently exceeding the current diffusion time or skin time.

Figure 1 shows the target area of JT-60SC above the experimental data on β_N achieved in various tokamaks in comparison with steady state reactor designs of SSTR [4], CREST [5] and ARIES [6], a non-inductive operation scenario of ITER [7], where the β_N values required from reactor designs are ranged from β_N=3.5-5.5. In response to the above requirements, it is necessary for the modification to incorporate superconducting toroidal and poloidal coils including renewal of main components such as vacuum vessel. However, the maximum utilization of existing facilities and equipments in JT-60 such as buildings, power supplies, heating equipments and diagnostics would significantly increase the advantage in cost and period for the modification.

Research issues for JT-60SC are summarized with target values based on conceptual reactor designs of SSTR and CREST emphasizing reactor economics as follows.

(i) Realization of high-beta steady-state operation:
high beta plasma control (β_N = 3.5 - 5.5),
steady state plasma control (f_{bs} = 50 - 90%),
diverter heat and particle control (f_{rad} ~95%, τ_{He}^*/τ_E ~ 5), and
disruption control (avoidance and mitigation).

(ii) Demonstration of the use of low-activation ferritic steel:
ideal MHD mode control with resistive and ferromagnetic wall,
locked mode and neoclassical tearing mode control with additional error fields, and
heat and particle control with plasma-material interaction,

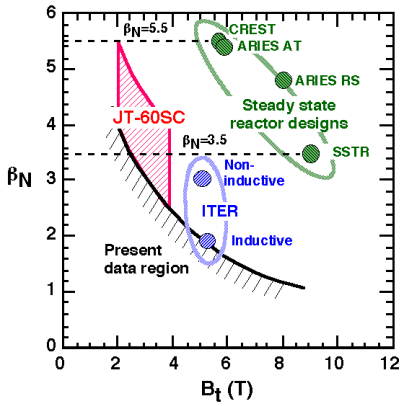

Fig.1. Normalized beta as a function of toroidal field showing the target area of JT-60SC along with reactor designs and the present experimental data region.

Table 1. Main parameters of JT-60U and JT-60SC

Parameter	JT-60U	JT-60SC
Pulse length	15 s	100 s (flat top)
Max. input power	40 MW (10 s)	44 MW (10 s)
		15 MW (100 s)
Plasma current I_p	3 MA	4 MA
Toroidal field B_t	4 T	3.8 T (R_p=2.8 m)
Major radius R_p	3.4 m	2.8 -3 m (2.8 m*)
Minor radius a_p	0.9 m	0.7-0.9 m (0.85 m*)
Elongation κ_{95}	1.8 (δ_{95}=0.06)	≤ 2 (1.8*)
Triangularity δ_{95}	0.4 (κ_{95}=1.33)	≤ 0.5 (0.35*)

* Nominal

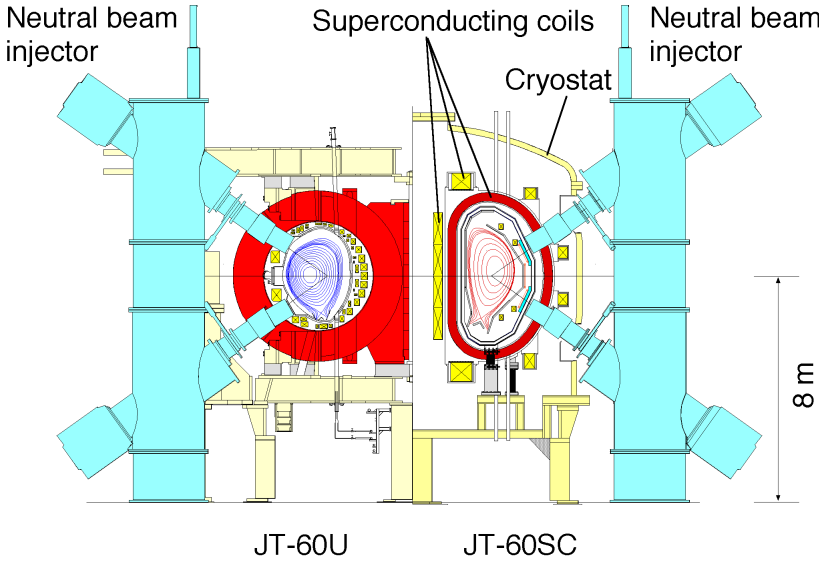

Fig.2. Comparison of cross-sectional views between JT-60U and JT-60SC.

where f_{bs} f_{rad}, τ_{He}* denote the bootstrap current fraction, the radiation fraction and the effective helium confinement time.

In response to the above requirements, main parameters of JT-60SC are defined nominally with the plasma current of 4 MA, the toroidal field of 3.8 T, the major radius of 2.8 m and the minor radius of 0.85 m as shown in Table 1 and a conceptual design is completed as shown in Fig. 2. Main heating equipments for JT-60SC are neutral beams capable of 40 MW/10 s or 13 MW/100 s (including negative ion beams: 10 MW/10 s or 3 MW/100 s) and electron cyclotron waves of 4 MW/10 s or 1.7 MW/100 s. Using the existing heating facilities, the JT-60SC is able to produce and sustain reactor-relevant plasmas for 100 s beyond the skin time τ_{skin} ~ 30 s in the range of ρ^* ~ 0.01 and ν^* ~ 0.01; Q_{DT}^{eq}=1.0 is projected for an inductive discharge with 4 MA, 3.8 T, P_{NB}=13 MW and $HH_{IPB(y,2)}$=1.18.

Figure 3 shows β_N as a function of the bootstrap current fraction illustrating the target area of JT-60SC, where full current drive data from high-β_p and reversed shear discharges in JT-60U [8,9,10,11], projections from SSTR, CREST and ITER are plotted. Typical results from the time-dependent transport simulations using the TOPICS code for JT-60SC are also plotted within the JT-60SC target area [12]. This shows that the attainment of high-β_N operation with a high bootstrap fraction under the full current drive condition is an important issue. In Fig.4, β_N is shown as a function of the ratio of the sustain duration of the high beta plasma to the skin time corresponding to the plots shown in Fig.3; where the skin time is simply defined as $\tau_{skin}=\mu_0 r^2/\eta$ around a half of minor radius. The necessity of long pulse experiments exceeding the skin time for the full current-drive high performance plasmas are clearly shown in Fig.4 in comparison with the JT-60U data. The target area of JT-60SC leading to reactor improvements has never been explored in any other tokamaks and is set beyond the scope of the ITER design for steady state operation.

3. Plasma Control Schemes

The eventual goal in JT-60SC is to achieve a comprehensive solution of the high-beta steady-state tokamak operation which is characterized by simultaneous attainments of sufficiently high confinement, normalized beta and bootstrap current fraction, efficient heat & particle control and almost disruption-free operation even in the use of the ferritic steel. On the way to the goal, the following physics issues are addressed with feasible plasma control schemes.

3.1 High Beta Plasma Control

Figure 5 shows the extended performance capability by the modification of JT-60 to JT-60SC

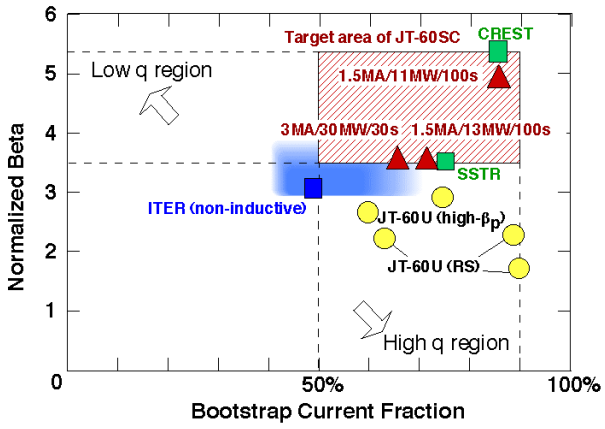

Fig.3. β_N as a function of bootstrap current fraction showing the target area and projections of JT-60SC along with SSTR, CREST and ITER in comparison with the data on full current drive discharges in JT-60U.

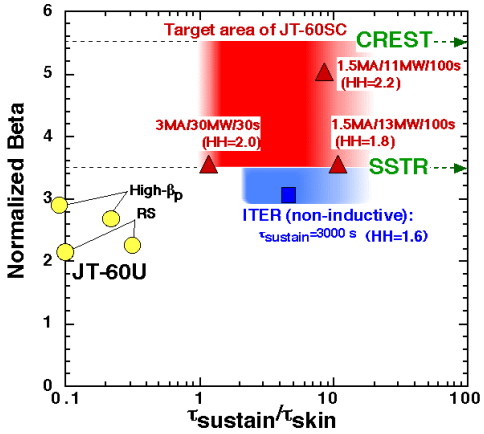

Fig.4. β_N as a function of the ratio of sustainment time to skin time showing the target area and projections of JT-60SC along with SSTR, CREST and ITER in comparison with the data on full current drive discharges in JT-60U.

to demonstrate the sustainment of high β_N plasmas in comparison with the present data from various tokamaks. CREST and SSTR are designed with β_N=5.5 and 3.5, respectively, well above no wall limit of ideal MHD instabilities. A non-inductive operation is aimed at β_N=3.1 in ITER.

As the target β_N range in JT-60SC is substantially above no wall MHD limit shown in Fig.6, the passive stabilizer plate made of the ferritic steel (F82H) is placed on the location similar to the blanket surface of a DEMO reactor; the JT-60SC plasma is approximately at r_{wall}/a~1.3. To stabilize resistive wall modes with multiple toroidal mode numbers of n=1 and 2 which could be unstable due to magnetic field penetration into the resistive wall, 18 sector coils are placed inside the vacuum vessel and behind the stabilizer plate, for active feedback control with fast response.

According to scaling laws for onset condition of neo-classical tearing modes (NTMs) [13], NTMs could be unstable in the required high beta plasmas and terminate the sustainment of the high β_N operation. Active and local electron cyclotron current drive (ECCD) technique becomes feasible for suppression of the NTMs by steering the launcher in combination with a high-resolution measurement (~ 1 cm) of the magnetic island since JT-60U has demonstrated the feedback stabilization of NTMs using the same techniques [14]. Time dependent NTM stability analysis combined with TOPICS and ECCD codes has been carried out for the JT-60SC plasma at 3 MA, showing that the NTMs can be suppressed by the present ECCD power of ~2 MW for 100 s and its decay time is reduced with decreasing the island width at which the ECCD is applied as show in Fig.7 [15].

3.2 Steady-State Plasma Control

Real time stabilization of the high beta plasma is planned with effective shaping, current/pressure and plasma rotation profile control capabilities using the poloidal field coils,

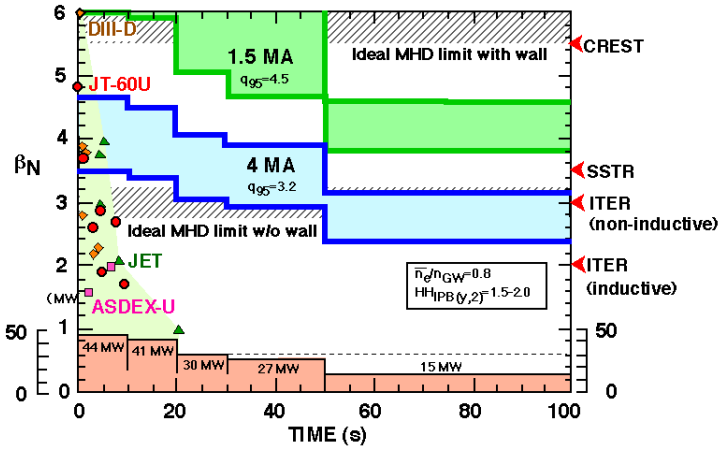

Fig.5. Attainable β_N as a function of time for various heating scenarios (44 MW/10 s, 41 MW/20 s, 30 MW/30 s, 27 MW/50 s, 15 MW/100 s) in JT-60SC along with the data on high beta achieved in tokamaks and the reference β_N values of SSTR, CREST and ITER.

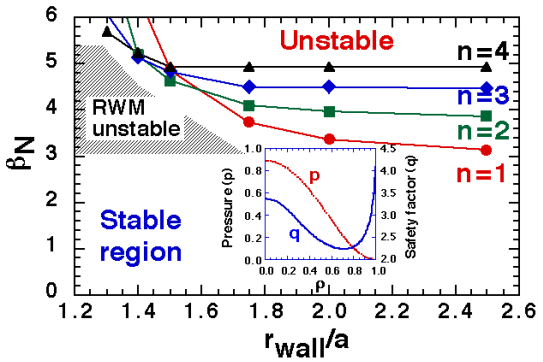

Fig.6. β_N as a function of normalized wall radius showing the beta limits for kink-ballooning modes with n=1 to 4 and possible resistive wall mode region along with the used pressure and current profiles.

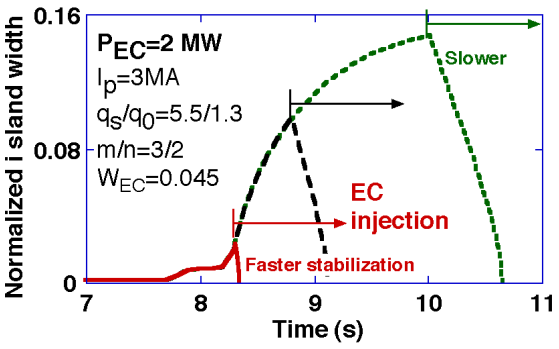

Fig.7. Temporal change of the normalized island width for three timings of ECCE onset showing different decay times of the island suppression.

a variety of beam arrangements in combination with central and off-axis, tangential and perpendicular injections with 90 and 500 keV, and steerable injection of 110 GHz EC wave from five gyrotrons.

Analyses based on high-β_p and reversed shear plasmas in JT-60U using TOPICS and ACCOME codes show the potential feasibility of high-beta steady-state operation for JT-60SC. As shown in Fig.8, the parameter scan for 3 MA discharges with 30 MW using the ACCOME code shows the wide range of full current drive capability including $HH_{IPB(y,2)}$ = 2.0, β_N = 3.5 and f_{bs} =65% with $n_{i0}\tau_E T_{i0}$=1x10^{21} keVsm^{-3}. The time dependent transport analysis using the TOPICS code shows the potential of high-beta steady-state operation at β_N~5 with f_{BS}~86% for 100 s as shown in Fig. 9 where the parameters are I_p=1.5 MA, B_t=2 T, $HH_{IPB(y,2)}$~2.2, P_{NB}=11 MW including N-NBI. The ERATO-J code analysis shows that the profiles with internal transport barrier could be stable for kink-ballooning modes.

3.3 Divertor Heat and Particle Control

Effective heat and particle control by the use of divertor is required as leading to simultaneous achievement of full current drive and partially detached divertor at high beta and reduction of impurity influx. The impurity control can be accomplished by a strong SOL flow produced by intense divertor pumping in combination with gas puff or high-field-side pellet injection. To ensure the heat and particle control including pulsed heat loads due to type I ELMs, the vertical target divertor is designed to be compatible with the elongated D-shaped equilibrium maintaining a sufficient SOL width of ~3 cm with a semi-closed divertor as shown in Fig.10 [16]. With the semi-closed divertor, the shaping control enables heat and particle control for the single null configurations with a large shift of the X-point and a wide expansion of the magnetic flux near the divertor region due to increase in the beta value. Independent pump-out scheme from inner and outer divertor slots using separated cryo-pumps is adopted for continuous partial detachment control: where the cryo-pump is capable of pumping out ~50 m^3/s at each slot based on numerical divertor simulation using the SOLDOR/NEUT2D code.

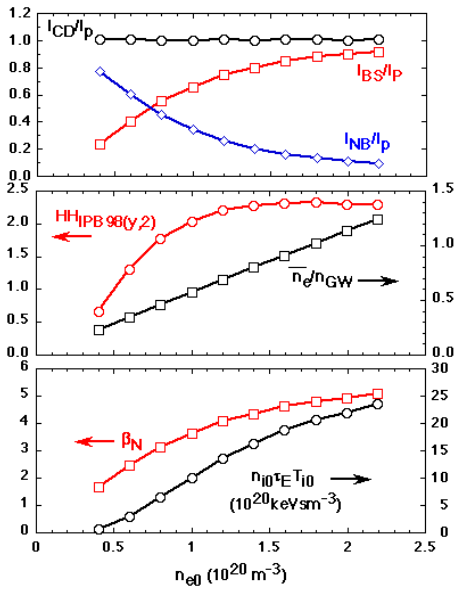

Fig.8. Non-inductive. bootstrap and beam-driven current fractions, HH-factor, normalized density and β_N and fusion tripple product as a function of the central density for full current drive condition from ACCOME code calculations at I_p=3 MA, B_t=3.8 T and P_{NB}=30 MW.

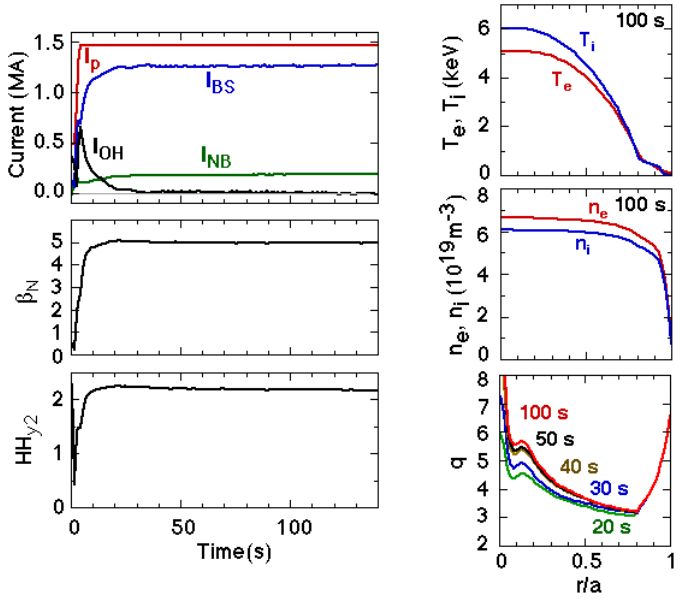

Fig.9. High-beta steady-state operation scenario sustained for 100 s from the TOPICS code analysis at I_p=1.5 MA, B_t=2.0 T and P_{NB}=11 MW, showing the temporal change of the plasma current, bootstrap current, beam current and OH current, bN and HH-factor and the profiles of T_e, T_i, n_e, n_i at 100 s and q at 20 s to 100 s.

Since the divertor heat load could reach ~20 MW/m^2 without any radiation loss, effective forced water cooling of the target plates is required as well as the radiative divertor formation. The material of divertor facing component will start from low-Z materials such as CFC including a local test of high-Z materials such as W-alloy towards the demonstration of divertor materials for DEMO reactors.

3.4 Effects of the Use of Ferritic Steel

The promising results from JFT-2M experiments using ferritic steel plates fully placed in the vacuum vessel [17] strongly support the use of ferritic steel in JT-60SC. In JT-60SC, ferritic steel is used for stabilizing baffle plates and first wall consisting of armors and pedestals so that the plasma is closely surrounded by the ferritic steel as shown in Fig.11. In JT-60SC, 18 TF coils generate magnetic fields with ripple rate up to 0.59% in the plasma region. To reduce the ripple rate in the ferritic steel configuration due to port hole arrangements, additional ferritic steel plates are appropriately installed inside the vacuum vessel behind the TFC. Consequently, the TF ripple rate of the 18 mode is reduced to down to 0.29% for plasma region over a wide range of B_t=2.0-3.8 T. The OFMC (Orbit Following Monte Carlo) code analysis to calculate fast ion losses indicates the effectiveness of ripple reduction where the fast ion loss for nearly perpendicular beams is evaluated to be 2.0% as shown in Fig.12.

Error fields induced by the ferritic steel are calculated on the plasma surface precisely including asymmetry and possible installation errors of the ferritic steel components; the Fourier spectrum of m= ± 2/n=1 are evaluated to be ~0.4 G. It is negligibly small in comparison with an onset level of locked mode, 7.6 G, at 3.8 T deduced from the result from DIII-D [18]. It is theoretically suggested that, with the presence of ferromagnetism in the wall material, the critical beta is reduced by ~10% with a wall thickness of 0.07a for μ/μ_0=2 at which the ferritic steel is sufficiently saturated [19]. Effect of flow velocity on the ideal MHD with resistive and ferromagnetic wall has been also investigated as shown in Fig.12, where the growth rates for both resistive and ideal wall branches are increased with permeability even with substantial flow velocity. These predictions should be elucidated in JT-60SC.

4. Superconducting Coils and Vacuum Vessel

Major components of the JT-60SC device are the superconducting coil system and the vacuum vessel containing a single-null elongated plasma, stabilizing baffle plates, first wall, a

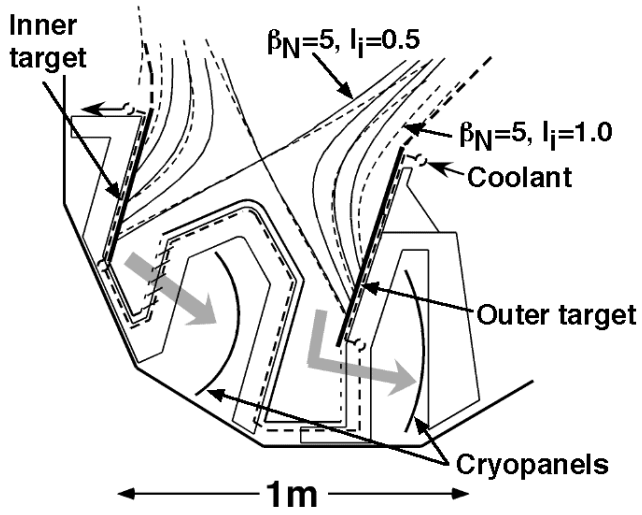

Fig.10. Concept of semi-closed vertical divertor with strong and separate pumping systems.

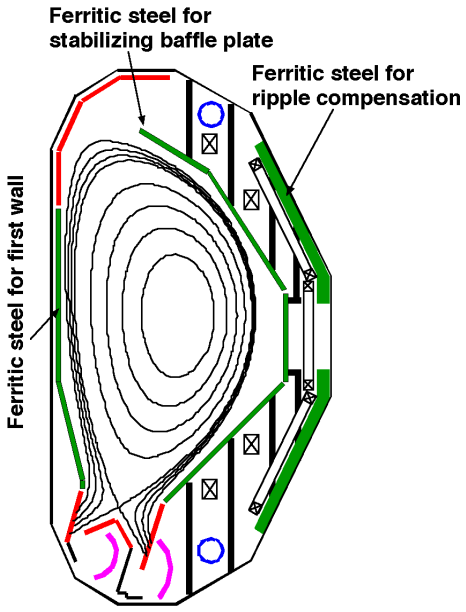

Fig.11. Invessel arrangements of ferritic steel used for first wall and stabilizing baffle plates, and for ripple compensation in the vacuum vessel.

vertical pumped divertor, fast position control coils and sector coils [20]. A cryostat encloses all the superconducting coils, the vacuum vessel and the support structures with thermal shields as shown in Fig.14.

The superconducting coil system consists of 18 toroidal field coils (TFC) and 10 poloidal field coils (PFCs) external to the TFC [21]. The PFC consists of 4 segments of the central solenoid (CS) and 6 equilibrium coils (EFCs). The TFC system produces 3.8 T at R_p=2.8 m with a maximum field of 7.4 T at winding and a magnetic stored energy of 1.7 GJ. A squired Nb_3Al cable-in-conduit conductor (CICC) using a stainless steel is a primary candidate for the TFC in JT-60SC, having the advantage of low strain sensitivity on superconducting performance allowing a react-and-wind technique and a high critical current density leading to a significant reduction of the amount of superconducting material [22]. Inboard side of the TFC cases is wedged against the centering force of the TFC. Inter-coil structures between the unit coils are provided to resist the toroidal forces as well as the centering force.

The PFC system provides a flux swing of 40 volt-seconds to inductively initiate the discharge and ramp up the plasma current up to 4 MA while leaving ~15 volt-seconds capable of sustaining the current flat top for 100 seconds at 4 MA without non-inductive current drive. The plasma is initiated by applying a toroidal electric field of 0.3 V/m with assistance of ECH. The CS is composed of 4 segment unit coils stacked in a support structure. A squired Nb_3Sn CICC using a stainless steel is used for the CS. The EF coil system consists of 6 coils, which are independently operated. The EFC for the bottom divertor coil uses the same conductor as the CS. Other EF coils are designed to use a squired NbTi CICC with a circular central channel for cooling, fabricated by a roll forming method [23].

The vacuum vessel is a double-walled structure with a polygonal shape having a low toroidal resistance of ~30 μΩ. The double walls made of low Co-contamination SS (SS316L) are filled with pure water for neutron shielding. Additionally, the SS316L boards are installed outside the vacuum vessel for γ-ray shielding. So that suppression of nuclear heating in the superconducting coils is established below 2.5 mW/cm^3 at coil winding. A neutron budget of 2×10^{20} neutrons/year is also established for JT-60SC based on 100 seconds of operation within 4×10^{17} n/s in deuterium. Vertical stability and kink stability for high beta plasmas can be achieved with passive structure of stabilizing baffle plates located inboard and outboard of the plasma. For slower growth of these instabilities, in-vessel copper coils to control horizontal and vertical fields and 18 sector coils to control helical magnetic field components

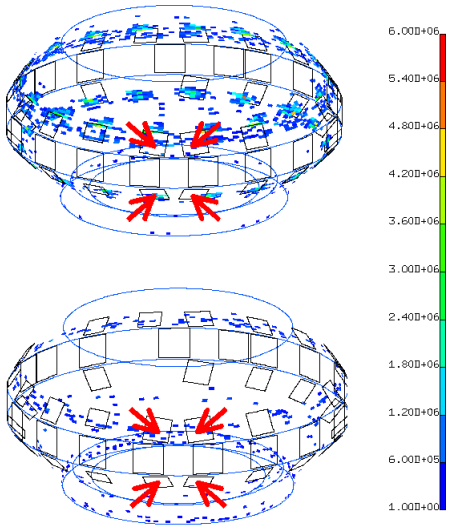

Fig. 12. 3D analysis fast ion losses (W/m^3) on the first wall taking into account port arrangements without (top) and with (bottom) ripple compensation by ferritic steel where arrows show the direction of nearly perpendicular beam injection.

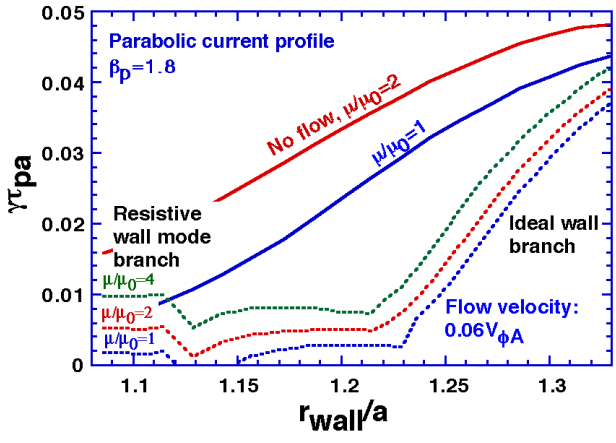

Fig. 13. Normalized growth rate as a function of normalized wall radius for permeability μ/μ_0=1, 2 (for JT-60SC), 4 of the resistive wall under substantial flow velocity in comparison with no flow case.

are installed as shown in Fig.11.

5. Summary

Objectives and design for the modification of JT-60 to a fully superconducting tokamak are defined and implemented, respectively, to realize high-beta steady-state operation in the use of low radio-activation ferritic steel towards improvements in economical and environmental attractiveness in tokamak reactors in national-wide collaboration with universities, institutes and industries in Japan. This planning is under discussion at governmental committees.

Acknowledgements

The authors appreciate contributions from the JT-60 Team, Superconducting Magnet Laboratory and NBI Heating Laboratory at JAERI.

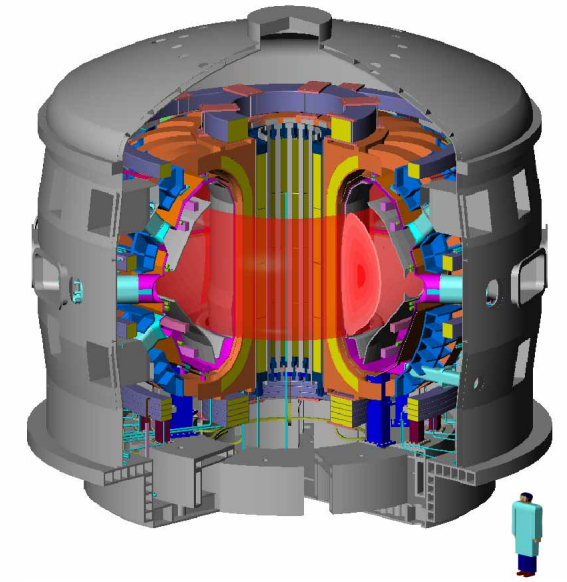

Fig.14. Bird's eye view of the JT-60SC device contained in the cryostat with a diameter of 12 m.

References

[1] J. D. Galambos et al., Nucl. Fusion 35(1995)551; K. Tokimatsu et al, Nucl. Fusion 38(1998)885.
[2] Y. Seki et al., Proc. 13th IAEA Conf. on Controlled Nuclear Fusion and Plasma Physics, Washington, 1990, IAEA-CN-53/G-1-2.
[3] S. Ishida et al., Proc. of 19th IEEE/NPSS Symposium on Fusion Engineering, Atrantic City 2002, p. 276.
[4] M. Kikuchi, Nucl. Fusion 30(1990)265
[5] K. Okano et al., Nucl. Fusion 40(2000)635.
[6] F. Najmabadi et al., 4th Int. Symo. on Fusion Technology, Tokyo April 1997.
[7] ITER Final Design Report, 2001.
[8] Y. Kamada et al., 15th IAEA Vol.1, p651 (1995);Y. Kamada et al., 16th IAEA Vol.1, p247 (1997).
[9] T. Fujita et al., Phys. Rev. Lett. 87, 085001 (2001).
[10] S. Ide et al., submitted to Plasma Phys. Contr. Fusion.
[11] Y. Takase et al., J. Plasma Fusion Res. 78(2002)719.
[12] H. Tamai, et al., in Proc. 29th EPS Conference on Plasma Phys. and Contr. Fusion (17-21 June 2002, Montreux, Switzerland) ECA Vol. 26B, P-1.050 (2002).
[13] ITER Expert Group on Disruptions, Plasma Control, and MHD, ITER Physics Basis Editors, Nucl. Fusion 39(1999)2251.
[14] A. Isayama et al., IAEA-CN-94/EX/C2-2.
[15] N.Hayashi et al., to be published in J. Plasma Fusion Res. Vol.5.
[16] S. Sakurai etal., Plasma Phys. Contorl. Fusion 44(2002) 749.
[17] Tsuzuki et al., IAEA-CN-94/EX/C1-1; K. Kamiya et al., IAEA-CN-94/EX/P2-05
[18] R.J. La Haye et al., Nucl. Fusion 32(1992)2119.
[19] G. Kurita et al., .IAEA-CN-94/FT/P1-06.
[20] T. Ando et al., Proc. 17th Int. Conf. on Magnet Technology, Jeneve, 2001, to be published in IEEE Tran. Appl. Supercond.
[21] A. Sakasai et al., IAEA-CN-94/FT/P2-09; A. Sakasai et al., Proc. of 19th IEEE/NPSS Symposium on Fusion Engineering, Atrantic City 2002, p. 221.
[22] K. Kizu et al., Proc. 17th Int. Conf. on Magnet Technology, Jeneve, 2001to be published in IEEE Tran. Appl. Supercond.
[23] Y. M. Miura et al., Proc. 17th Int. Conf. on Magnet Technology, Jeneve, 2001, to be published in IEEE Tran. Appl. Supercond.